Available online at www.sciencedirect.com

SciVerse ScienceDirect

Procedia Engineering 00 (2012) 000–000

Procedia Engineering

www.elsevier.com/locate/procedia

5th BSME International Conference on Thermal Engineering

A review of flow and heat transfer in rotating microchannels

Pratanu Roy[a], N.K. Anand[a,*], Debjyoti Banerjee[a]

[a]*Department of Mechanical Engineering, Texas A&M University, College Station, TX 77840, USA*

Abstract

Rotating microchannels are integral part of centrifugally actuated miniaturized microfluidic devices, which have important applications in chemical analysis and biomedical diagnostics. As the field of centrifugal microfluidics continues to evolve, it is becoming imperative to understand the fundamental principles of fluid flow inside microchannels under the influence of centrifugal and Coriolis forces. These forces arise as a consequence of expressing the governing equations in rotating Eulerian reference frame and change the flow pattern significantly from the symmetric parabolic profile of a non-rotating channel. In this paper, we have summarized the recent advances in the area of fluid flow and heat transfer applications in radially rotating microchannels. A review of experimental and numerical studies available in the current literature is performed and issues with the applicability of analytical correlations for conventional macro-sized channels to describe the microscale flow phenomena have been discussed. From this state of the art review, it is evident that further systematic investigations are needed for a clear understanding of the transport mechanism associated with the flow and heat transfer inside rotating microchannels.

Keywords: Rotating microchannels; Centrifugal microfluidics; Secondary flow; Centrifugal force; Coriolis force.

Nomenclature

a	Width of the microchannel (m)	u_j	Velocity in j-direction (u, v, w for j = 1,2,3)
b	Height of the microchannel (m)	u,v,w	Velocities in x,y and z directions (m/s)
D_h	Hydraulic diameter of the microchannel (m)	x_i	Co-ordinates in i-direction (x, y, z for i = 1,2,3)
d_r	Radial distance of inlet from disk center (m)	*Greek Symbols*	
f_c	Coriolis force (N/ m^3)	α	Aspect ratio (= a/b)
f_ω	Centrifugal force (N/m^3)	β	Ratio of Coriolis force to centrifugal force
k	Thermal conductivity (W/m-K)	μ	Dynamic viscosity of fluid (Pa-s)
Kn	Knudsen number	ω	Rotation or angular velocity (rad/s)
L	Length of the microchannel (m)	*Subscripts*	
p	Pressure (Pa)	*avg*	Average
Re	Reynolds number	*cr*	Critical
Re_ω	Rotational Reynolds number	*i, j, k*	Array indices for tensor notation
RPM	Revolution per minute	*max*	Maximum
S_j	Source term in j-direction		
T	Temperature (^{o}C)		

* Corresponding author. Tel.: +1-979-845-5633; Fax: +1-979-845-4925.
E-mail address: nkanand@tamu.edu

1. Introduction

Investigation of fluid flow and heat transfer in rotating microchannels is important for centrifugally actuated microfluidic devices, which have enormous potential in the field of chemical analysis, drug delivery and biomedical applications. In these devices, an array of microchannels is etched on a compact-disk like circular substrate, which is then rotated at a certain frequency. By controlling the rotating frequency, various liquid handling processes, such as mixing, separation, routing, valving, siphoning, and droplet generation can be performed efficiently [1, 2]. This kind of arrangement is popularly known as *Lab-on-a-CD* or *LabCD* [1-3]. The objective of this compact disk like platform is to combine multiple liquid handling steps in order to perform all the bio-chemical processes in a flexible way [4].

A successful design of centrifugal microfluidic devices requires a clear understanding of fluid flow inside rotating microchannels. The physics of fluid flow through rotating microchannels is primarily governed by the pseudo forces, namely the centrifugal and the Coriolis forces, arising as a consequence of expressing the governing equations in rotating reference frame. At low rotation speed, the flow is purely driven by the centrifugal force. At higher rotation, the Coriolis force becomes dominant and a significant secondary flow can be observed perpendicular to the primary flow velocity. The effective operation of a centrifugal microfludic platform depends on regulating these forces in a controlled manner. For example, the working principle of capillary burst valve depends on the balance of centrifugal force and surface tension force [5]. On the other hand, mixing is enhanced in microchannels when the Coriolis force dominates over the centrifugal force [6]. The process becomes more complicated when heat transfer is included in the scenario. In some cases it is necessary to maintain the fluid within specific temperature ranges while rotating it inside the microchannel. For instance, the polymerase chain reaction (PCR) needs thermal homogeneity for efficient DNA hybridization [7]. In order to compute the correct temperature distribution of the fluid inside a rotating microchannel, the effect of rotation on convective heat transfer should be taken into consideration.

The flow physics in microscale can be modeled in two ways – one is by assuming it as a continuous medium with spatial and temporal variations of macroscopic flow quantities such as velocity, pressure, temperature or density and the other is by treating it as a collection of discrete particles whose flow properties are obtained by deterministic or probabilistic approaches [8]. The validity of Navier-Stokes equations to adequately describe the physics of flow inside microchannels depends upon the continuum hypothesis. Knudsen number (Kn), which is the ratio of the mean free path of the fluid molecules to the characteristic length, is often used as a validity indicator of the continuum hypothesis assumption [8-10]. For $Kn < 0.01$, the fluid can be considered as a continuum. As the Knudsen number approaches unity the continuum equations begin to fail, but for $Kn < 0.1$ the no slip boundary condition can still be adjusted using a slip parameter. The region ($0.01 < Kn < 0.1$) is called the "slip regime", to distinguish it from the transition regime ($0.1 < Kn < 10$), in which the Boltzmann equations are solved directly to predict flows.

For biological liquids, such as blood, plasma, urine, and for water, Knudsen number (Kn) falls well within the continuum region, where Navier-Stokes equations with no slip boundary conditions are applicable for any practical range of microchannel size. However, even for water flow in microchannels, contradictory results on the validity of the Navier-Stokes equations have been reported in the literature. Garimella and Sobhan [11] conducted a comparative study on the transport in microchannels and concluded that analyses based on Navier-Stokes and energy equations can adequately predict the flow and heat transfer characteristics in microchannel having a hydraulic diameter greater than 50 μm, provided that the experimental conditions and measurements are correctly identified and simulated. Another critical review on single phase liquid friction factors in microchannels was performed by Steinke and Kandlikar [12]. By analyzing over 150 papers that directly deal with the pressure drop measurements in the microchannels, they generated a database of over 5000 data points with the Reynolds number ranging from 0.002 to 5000 and hydraulic diameter ranging from 8 μm to 990 μm. They argued that, the studies which reported a deviation of friction factor from conventional theory did not account for the developing region or exit effect in the microchannel. Therefore, it was concluded that, the classical correlations are reliable in predicting the flow and heat transfer phenomena in microchannel as long as the entrance or exit effect and the experimental uncertainties are taken into account.

If the continuum hypothesis is also valid for centrifugally driven micro-flows, then the analysis of flow and heat transfer will not differ from that in rotating macro sized channels. In this article, we will focus on how the fluid flow and heat transfer characteristics inside rotating microchannels are used in the area of centrifugal microfluidics. Section 2 presents the recent reviews and trend of centrifugal microfluidics. Section 3 describes the working principle of a typical centrifugal microfluidic platform. Various applications of rotating microchannels in centrifugal microfluidics have been discussed in section 4. The final section summarizes the review and briefs about the future recommendations on this topic.

2. Recent literature review

Figure 1 shows the number of papers containing the term *centrifugal microfluidics* in the recent years. The results were compiled using the database of Web of Science, Elsevier, MEDLINE, IOP Electronic Journals, Health Reference Center

Academic, Directory of Open Access Journals, BioMed Central and American Chemical Society. Over the past decade, a steady increase of interest on the topic of centrifugal microfluidics can clearly be observed.

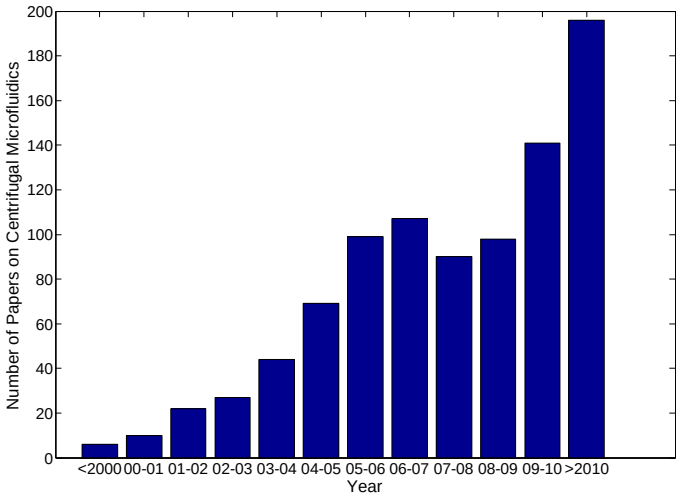

Fig. 1. Growth of publications on centrifugal microfluidics in the recent years

Comprehensive reviews on centrifugal microfluidics for biomedical applications can be found in [1, 13]. These reviews highlighted the recent progress in the relevant field and outlined the potential for future applications. Another review on centrifugal microfluidic and bio-optical disks can be found in [14]. The present review will emphasize on the more recent advances on centrifugal microfluidics. Selected literatures on the applications of centrifugal microfluidics are given in Appendix A.

3. Working principle

In most of the centrifugal microfluidic devices, the fluid is placed in a microchamber, which is connected to another reservoir through a microchannel. Figure 2 shows a schematic diagram of an array of rectangular microchannels aligned radially on a circular disk and a single microchannel on a rotating disk with corresponding forces acting on the flow. As the disk is rotated around an axis perpendicular to the plane of the disk, a centrifugal force f_ω is induced in the radially outward direction and the liquid advances through the microchannels towards the outlet. At this stage, the velocity of the liquid and the shape of the liquid meniscus are primarily governed by the centrifugal force and the surface tension force. Once the microchannel is filled up with the liquid, a continuous stream of liquid flow is established along the microchannel and the surface tension effect can be neglected. Due to the rotation, a Coriolis force f_c is also induced perpendicular to the centrifugal force on the disk plane. This Coriolis force is responsible for generating secondary flow phenomena in rotating microchannel flow.

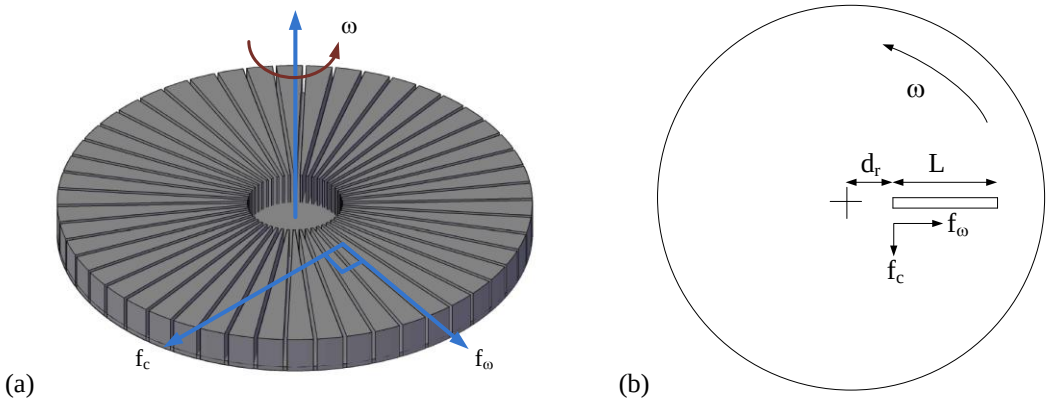

Fig. 2. Schematic of working principle : (a) an array of microchannels (b) simplified rotating disk with a single microchannel

If an unsteady, laminar, incompressible flow with constant thermo-physical properties and negligible buoyancy force is assumed, then the governing equations for microchannel flow with a generic forcing term S_j, can be written in the following Cartesian tensor form:

Continuity: $$\frac{\partial u_i}{\partial x_i} = 0 \quad (1)$$

Momentum: $$\rho\left(\frac{\partial u_j}{\partial t} + u_i\frac{\partial u_j}{\partial x_i}\right) = -\frac{\partial p}{\partial x_j} + \mu\left(\frac{\partial^2 u_j}{\partial x_i \partial x_i}\right) + \rho S_j \quad (2)$$

Energy: $$\rho C_p\left(\frac{\partial T}{\partial t} + u_i\frac{\partial T}{\partial x_i}\right) = \frac{\partial}{\partial x_i}\left(-k\frac{\partial T}{\partial x_i}\right) \quad (3)$$

For i, j = 1, 2, 3, $x_1 \in (0, a), x_2 \in (0, b), x_3 \in (0, L)$. Here, a, b and L are the width, height and length of the channel respectively. If we consider Cartesian velocity components u, v, w in x, y, z directions in place of u_1, u_2, u_3 velocities in x_1, x_2, x_3 directions, then the source terms in the momentum equations for an orthogonal rotation mode becomes [15]:

x-direction: $$S_1 = -2\omega w + \omega^2 x \quad (4)$$

y-direction: $$S_2 = 0 \quad (5)$$

z-direction: $$S_3 = 2\omega u + \omega^2(d_r + z) \quad (6)$$

Two non-dimensional numbers, namely flow Reynolds number (*Re*) and rotational Reynolds number (Re_ω) characterize the physics of rotating channel flows. Reynolds number ($Re = \rho w_{avg} D_h/\mu$) is the ratio of the inertial force to viscous force and rotational Reynolds number ($Re_\omega = \rho\omega D_h^2/\mu$) is the ratio of the rotating force to the viscous force. If a parabolic axial velocity profile is assumed in the primary flow direction, then it can be shown that the axial velocity (w) is in the order of ($\sim\rho\omega^2 D_h^2 d_r/8\mu$) [16]. Thus, the ratio of the Coriolis force $(2\rho\omega w)$ and the centrifugal force $(\rho\omega^2 d_r)$ becomes $\beta=\rho\omega D_h^2/8\mu$, which is a multiple of rotational Reynolds number Re_ω. This indicates that, a high rotational Reynolds number will induce high Coriolis force resulting in a strong secondary flow.

4. Review of rotating microchannel applications

In this section we present a review of the recent applications of rotating microchannel in centrifugal microfluidics area.

4.1. Centrifugal pumping

Centrifugal pumping occurs when the liquid flows from the reservoir into the microchannels due to the centrifugal force (as described in section 3). Duffy et al. [17] measured the experimental flow rate during centrifugal pumping inside microchannels of different widths (20 – 500 μm), depths (16 – 340 μm), and lengths (12.5-182 mm) subjected to a range of rotational frequencies (400-1600 RPM). They compared the experimental flow rate with the Hagen-Poiseuille flow rate in a log-log graph and showed that centrifugally driven microchannel flows can be treated as Hagen-Poiseuille flows for a wide range of attributes. Madou et al. [18] measured the pressure drop against the flow rate relationship for two different microchannels (one 150 μm wide and 34 μm deep, and the other 50 μm wide and 34 μm deep). They also showed that the flow rate *Q* can be predicted with Hagen-Poiseuille equation: $Q = \pi D_h^4 \Delta P/128\mu L$. For a purely centrifugal flow, the pressure difference ΔP between the channel inlet and outlet can be expressed by: $\Delta P = \rho\omega^2 r_{av}\Delta r$. Sine, $Q = w_{avg}A$, the average velocity $w_{avg} = \rho\omega^2 r_{av}\Delta r D_h^2/32\mu L$. Here, r_{av} is the average distance of the liquid from the disk center and Δr is the radial extent of the fluid. For rectangular microchannels, a better approximation for velocity can be derived by neglecting the non-linear convective terms and Coriolis force terms in the Navier-Stokes equations and then solving the resulting Poisson equation with a modified pressure-gradient [19]. All these approximations may work well for low rotational Reynolds number ($Re_\omega \sim O(1)$). However, for high rotational Reynolds number, the Coriolis force can change the velocity profile significantly from these relations and then the effect of secondary flow should be taken into account.

In order to illustrate how the flow in centrifugal pumping are affected by the rotation, the steady state governing equations were solved numerically for radially rotating rectangular microchannels of different aspect ratios ($\alpha = a/b$) with hydraulic diameter D_h = 200μm and Re = 100. The details of the numerical solver used for the simulation can be found in [20]. Figure 3 presents the deviation of the friction relation of a rotating channel flow from that of a non-rotating channel flow. The friction factor (*f*) or the friction relation (*fRe*) can be considered a measure of the pumping power required to drive the centrifugal flow. From Figure 3, it can be observed that, as the rotational speed (RPM) or the rotational Reynolds number (Re_ω) increases, the percentage deviation of the friction relation of a rotating channel flow from that of a non-

rotating channel flow increases. Moreover, for a fixed rotational Reynolds number, this deviation is low for wide aspect ratio channels, whereas the deviation is high for low aspect ratio channels. It indicates that, for rectangular channels, channel height might be a better representative of the characteristic length than the hydraulic diameter.

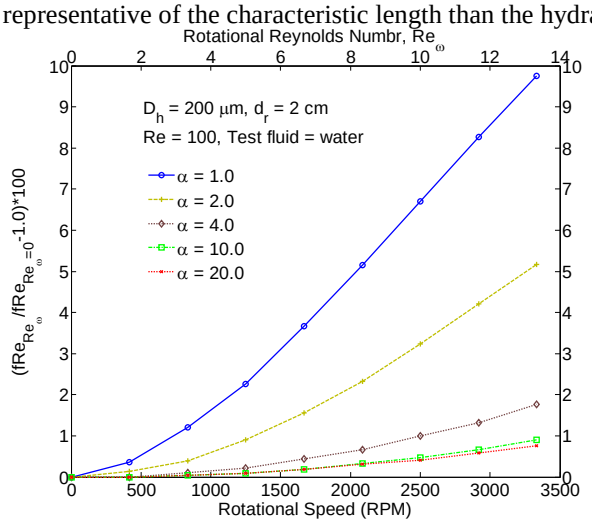

Fig. 3. Deviation of friction relation *(fRe)* of rotating microchannels from that of non-rotating microchannels

In practice, for microfluidic devices, it is not possible to simultaneously control both the rotational speed and Reynolds number. In most of the centrifugal microfluidics devices, the fluid is kept in a reservoir and the disk is rotated at a certain rotating frequency. As a result, fluid from reservoir flows through the microchannel due to the centrifugal force just like a pressure driven flow occurs due to the pressure difference at channel inlet and outlet. Once the rotating frequency is fixed, the velocity (and the Reynolds number) of the fluid inside the microchannel is also fixed. Thus, the rotating speed and the Reynolds number or fluid velocity is coupled in a centrifugally driven flow. In order to account for this coupled nature, the average velocity of the fluid was calculated using the analytical solution of a purely centrifugal flow in rectangular channel with zero pressure-gradient [21]. Figure 4 presents the comparison of velocity profiles of steady rotating channel flows with the analytical results for different rotational Reynolds number. By inspecting this figure, it can be observed that, for low rotational Reynolds number (Re_ω = 1.67, RPM = 400), the velocity profiles are very close to the analytical results. However, for large rotational Reynolds number (Re_ω = 17.86, RPM = 4200), the velocity profiles deviate significantly from the symmetric parabolic flow profiles proposed by the analytical solutions. Thus, although the existing analytical solutions of centrifugal flow can be used to predict the flow parameters, care should be taken to consider the uncertainty introduced by these approximations at large rotational Reynolds number.

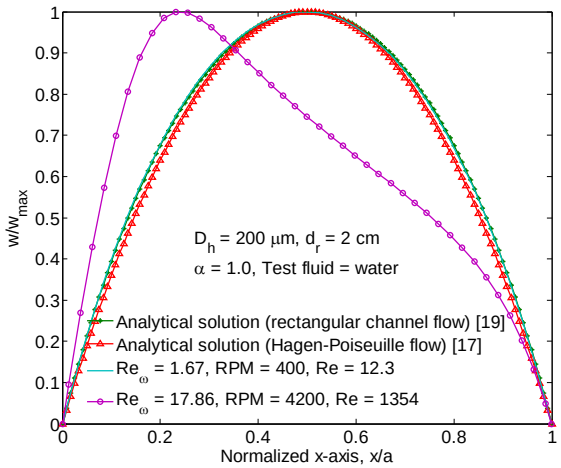

Fig. 4. Comparison of outlet velocity profiles of rotating microchannels with approximate analytical solutions

4.2. Mixing

Due to the small length scale of microfluidic devices, the Reynolds number is typically in the laminar flow regime. As a result, mixing in microscale is primarily dominated by diffusion process, which is time-consuming. In centrifugal microfluidic platform, rapid mixing can be achieved by alternate rotation (clockwise and counter-clockwise) of the microchambers containing the mixture [22, 23]. The mixing process can be further enhanced by pre-filling the mixing chambers with paramagnetic beads and placing a permanent magnet underneath it to induce a magnetic stirring [22, 24, 25]. An alternative approach to these methods is to induce strong secondary flow resulting from Corolis force at high rotational speeds [6, 16]. In a recent study on the characteristics of two fluid mixing in rotationally actuated T-shaped microchannel, Chakraborty et al. [26] identified three distinct mixing regimes based on the change of mixing patterns with the change of β. The three regimes are – (i) diffusion based mixing (at low rotation speeds, $0 < \beta < 1.0$), (ii) Coriolis force based mixing (at intermediate rotation speeds, $1.0 < \beta < 2.0$), and (iii) mixing based on flow instability (at high rotation speeds, $\beta > 2.0$). It is interesting to note that, although Coriolis force based mixing regime starts at $\beta = 1.0$, the efficient mixing occurs when β exceeds 1.35 that is when $Re_\omega > 10.8$. From the definition of rotational Reynolds number Re_ω,it can be seen that, Re_ωvaries with the square of the hydraulic diameter D_h. Thus, to attain an effective Coriolis based mixing, one should choose relatively large scale channel dimensions so that Re_ω is sufficiently high to impact the transverse flow.

By solving the governing equations numerically, we can determine for what values of rotational Reynolds number the effect of rotation is significant. Figure 5 shows the variation of friction relations for rotating microchannels in comparison to non-rotating microchannels for a range of Reynolds number and rotational Reynolds number. The case with aspect ratio α = 9.09 corresponds to the geometry used in the experiment of Chakraborty et al. [26]. From this graph, it can be seen that, as the rotational Reynolds number increases, the secondary flow effect increases and the friction factor deviates from the value of its non-rotating counterpart. From the numerical data, it was found that, one percent deviation in friction relation produces a secondary flow in an amount of 2-3% of the average velocity. In case of low rotational speed, the centrifugal flow has low Reynolds number and consequently the secondary flow will be negligible. But, high rotational speed will result in a high Reynolds number flow which will in turn induce a large secondary flow. If 1% deviation in *fRe* is considered as a critical value above which the effect of Coriolis force will be significant, then a demarcation line can been drawn in Figure 5 to differentiate between the diffusion dominated region and secondary flow dominated region. A corresponding critical value for rotational Reynolds number ($Re_{\omega,cr}$) can be derived from the diagram. For α = 9.09, $Re_{\omega,cr} = 10.2$, which is very close to the value reported by Chakraborty et al. ($\beta = 1.35$, $Re_\omega = 10.8$) [26]. For other aspect ratios, critical rotational Reynolds number can be derived in a similar way.

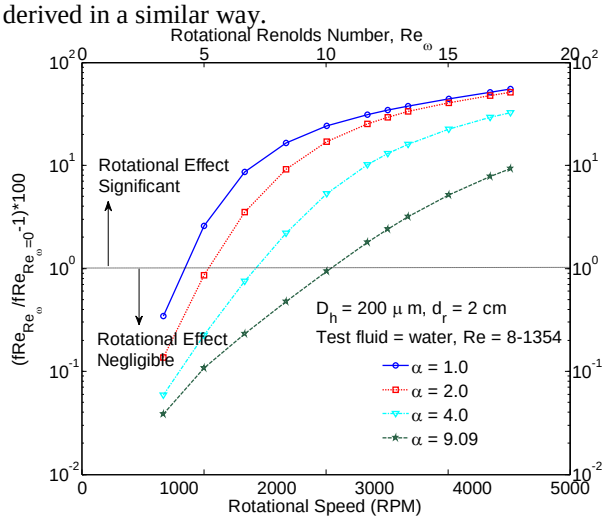

Fig. 5. Identification of significant secondary flow dominant regions and critical rotational Reynolds number

Other methods of mixing in rotating microchannels have also been reported. Micromixing of liquids by pneumatic agitation on centrifugal microfluidic platform was recently reported by Kong et al. [27]. A stream of compressed gas was applied to agitate the liquids and a 30-fold improvement in mixing was observed over a range of rotational frequencies (450-1500 RPM) compared to the conventional diffusion-based mixing.

4.3. Valving

By exploiting the capillary effect and the wetting nature of the channel surface, passive microfluidic valve can be constructed without any moving parts. Capillary valves are operated using the developed pressure barrier when the capillary flow channel undergoes a sudden expansion in cross-section [5]. Figure 6a demonstrates a capillary valve, where the bursting frequency depends on the balance between surface tension induced pressure and centrifugally induced pressure [13]. The critical burst condition refers to the condition when the centrifugally induced pressure reaches the surface tension induced pressure and the capillary valve opens. By balancing these two pressures a simple analytical relation among critical (bursting) frequency (ω_{cr}), surface tension (σ) and characteristic length (D_h) can be deduced: $\rho\omega_{cr}^2 r_{av}\Delta r > 4\sigma/D_h$ [5, 28-30].

Depending on the wetting nature of the surface, the microchannel surface can be either hydrophilic or hydrophobic. A hydrophilic surface has a strong affinity to water with a contact angle less than 90^o. On the other hand, due to large contact angles ($>90^o$) and the repelling nature of a hydrophobic surface, water do not stick to it. Capillary bust valves are made of hydrophilic microchannels. Another type of valving used in centrifugal microfluidics is hydrophobic valving, where a small hydrophobic channel is placed right after the microchamber to restrict the fluid movement (refer to Figure 6b) [2].

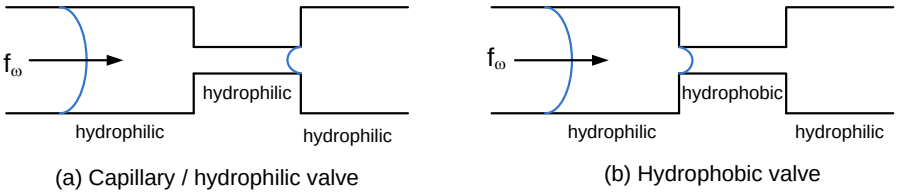

(a) Capillary / hydrophilic valve (b) Hydrophobic valve

Fig. 6. Schematic of: (a) Capillary valve (b) Hydrophobic valve (Redrawn from [2])

4.4. Directional Switching

In a rotating microchannel, the effect of Coriolis force is to generate a transverse velocity component perpendicular to the main flow direction, the sign of which depends on the sense of rotation. The transverse or secondary flow can be used to generate directional switching at high spinning frequencies [31-33]. Figure 7 shows an example of directional switching in Y-shaped structure, which is also known as 'passive flow switching valve' [32].

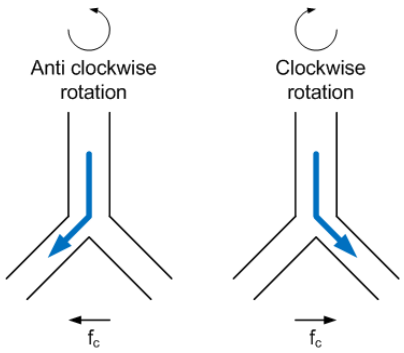

Fig. 7. Directional switching based on Coriolis force and sense of rotation (adapted from [23])

Another form of flow switching on centrifugal microfluidic platform can be achieved by using a regulated stream of compressed gas. Kong et al. [34] implemented this technique to control the flow at a T-junction for relatively low rotational frequencies (400-1200 RPM).

4.5. PCR Amplification

During Nucleic acid (NA) analysis, a common step is to amplify Polymerase Chain Reaction, or PCR. This requires repeated thermocycling of the analyte NA in a microchamber [7] i.e. the reaction volume is maintained under prescribed temperature zones, typically 90^o-94^oC for denaturation (that causes DNA melting by disrupting the hydrogen bonds), 50^o-70^oC for renaturation (i.e. annealing) and 70^o-90^oC for extension. By using the secondary flow effect, thermal homogeneity can be achieved in PCR amplification on a spinning disk. Aamsia et al. [35] demonstrated an automated centrifugal

microfluidic system for PCR amplification using novel thermoelectric heating and ice-valves. Seigrist et al. [7] numerically and experimentally analyzed the rotating PCR microchamber filling behavior at different inlet pressure boundary conditions (0.5 kPa to 2.0 kPa). They showed that, due to the induced centrifugal and Coriolis force, the nature of chamber filling is different for rotating case from that of non-rotating case.

5. Summary

In this paper, we have summarized the recent advances in the applications of radially rotating microchannels. A review of experimental and numerical studies available in the current literature was performed. The applicability of analytical correlations for conventional macro-sized channels to describe the rotating microchannel flow phenomena has been discussed. Numerical results showed that, for low rotational Reynolds number, the effect of Coriolis force is small and the existing analytical solutions for fully developed pipe or channel flow can be used. However, for high rotational Reynolds number, the deviation of flow parameters in rotating microchannel flow can be significant and the uncertainty introduced by using the analytical results can be high. By comparing the friction relation of a centrifugally driven flow from that of a non-rotating channel flow, a critical rotational Reynolds number ($Re_{\omega,cr}$) can be identified, above which the effect of rotation is significant. However, a clear picture of flow regimes showing where the secondary flow effect is considerably high is still missing. Thus, it is evident that further systematic investigations are needed to find out the range Reynolds number (Re) and rotational Reynolds number (Re_{ω}), for which the secondary flow inside rotating microchannels can be considered significant.

References

[1] Madou, M., Zoval, J., Jia, G., Kido, H., Kim, J., and Kim, N., 2006, "Lab on a Cd," Annu. Rev. Biomed. Eng., 8(pp. 601-628.
[2] Ducrée, J., Haeberle, S., Lutz, S., Pausch, S., Von Stetten, F., and Zengerle, R., 2007, "The Centrifugal Microfluidic Bio-Disk Platform," Journal of Micromechanics and Microengineering, 17(7), pp. S103.
[3] Madou, M. J., and Kellogg, G. J., 1998, "The Labcd: A Centrifuge-Based Microfluidic Platform for Diagnostics," Proc. Systems and Technologies for Clinical Diagnostics and Drug Discovery, Vol. 3259, pp. 80-93.
[4] Mark, D., Haeberle, S., Roth, G., Von Stetten, F., and Zengerle, R., 2010, "Microfluidic Lab-on-a-Chip Platforms: Requirements, Characteristics and Applications," Chem. Soc. Rev., 39(3), pp. 1153-1182.
[5] Zeng, J., Banerjee, D., Deshpande, M., Gilbert, J. R., Duffy, D. C., and Kellogg, G. J., 2000, "Design Analyses of Capillary Burst Valves in Centrifugal Microfluidics," μTAS 2000 Symposium, Enschede, Netherlands, May 14-18, 2000.
[6] Ducrée, J., Haeberle, S., Brenner, T., Glatzel, T., and Zengerle, R., 2006b, "Patterning of Flow and Mixing in Rotating Radial Microchannels," Microfluidics and Nanofluidics, 2(2), pp. 97-105.
[7] Siegrist, J., Amasia, M., Singh, N., Banerjee, D., and Madou, M., 2010, "Numerical Modeling and Experimental Validation of Uniform Microchamber Filling in Centrifugal Microfluidics," Lab Chip, 10(7), pp. 876-886.
[8] Gad-El-Hak, M., 1999, "The Fluid Mechanics of Microdevices-the Freeman Scholar Lecture," Transactions - ASME Journal of Fluids Engineering, 121(pp. 5-33.
[9] Gad-El-Hak, M., 2002, *The Mems Handbook*, CRC Pr I Llc,
[10] Bontemps, A., 2005, "Measurements of Single-Phase Pressure Drop and Heat Transfer Coefficient in Micro and Minichannels," Microscale Heat Transfer Fundamentals and Applications, pp. 25-48.
[11] Garimella, S. V., and Sobhan, C., 2003, "Transport in Microchannels–a Critical Review," Ann. Rev. Heat Transfer, 13(pp. 1–50.
[12] Steinke, M. E., and Kandlikar, S. G., 2006, "Single-Phase Liquid Friction Factors in Microchannels," International journal of thermal sciences, 45(11), pp. 1073-1083.
[13] Gorkin, R., Park, J., Siegrist, J., Amasia, M., Lee, B. S., Park, J. M., Kim, J., Kim, H., Madou, M., and Cho, Y. K., 2010, "Centrifugal Microfluidics for Biomedical Applications," Lab Chip, 10(14), pp. 1758-1773.
[14] Nolte, D. D., 2009, "Invited Review Article: Review of Centrifugal Microfluidic and Bio-Optical Disks," Review of Scientific Instruments, 80(10), pp. 101101-101101-22.
[15] Morris, W. D., 1981, *Heat Transfer and Fluid Flow in Rotating Coolant Channels*, Research Studies Press,
[16] Ducree, J., Brenner, T., Haeberle, S., Glatzel, T., and Zengerle, R., 2006, "Multilamination of Flows in Planar Networks of Rotating Microchannels," Microfluidics and Nanofluidics, 2(1), pp. 78-84.
[17] Duffy, D. C., Gillis, H. L., Lin, J., Sheppard Jr, N. F., and Kellogg, G. J., 1999, "Microfabricated Centrifugal Microfluidic Systems: Characterization and Multiple Enzymatic Assays," Analytical Chemistry, 71(20), pp. 4669-4678.
[18] Madou, M. J., Lee, L. J., Daunert, S., Lai, S., and Shih, C. H., 2001, "Design and Fabrication of Cd-Like Microfluidic Platforms for Diagnostics: Microfluidic Functions," Biomedical Microdevices, 3(3), pp. 245-254.

[19] Chakraborty, D., Gorkin, R., Madou, M., Kulinsky, L., and Chakraborty, S., 2009, "Capillary Filling in Centrifugally Actuated Microfluidic Devices with Dynamically Evolving Contact Line Motion," Journal of Applied Physics, 105(8), pp. 084904-084904-10.
[20] Roy, P., Anand, N. K., and Banerjee, D., 2011, "A Numerical Study of Unsteady Laminar Flow and Heat Transfer through an Array of Rotating Rectangular Microchannels," ASME Conference Proceedings, 2011(54921), pp. 1141-1145.
[21] Liu, M., Zhang, J., Liu, Y., Lau, W., and Yang, J., 2008, "Modeling of Flow Burst, Flow Timing in Lab-on-a-Cd Systems and Its Application in Digital Chemical Analysis," Chemical Engineering & Technology, 31(9), pp. 1328-1335.
[22] Grumann, M., Geipel, A., Riegger, L., Zengerle, R., and Ducree, J., 2005, "Batch-Mode Mixing on Centrifugal Microfluidic Platforms," Lab on a Chip, 5(5), pp. 560-565.
[23] Noroozi, Z., Kido, H., Micic, M., Pan, H., Bartolome, C., Princevac, M., Zoval, J., and Madou, M., 2009, "Reciprocating Flow-Based Centrifugal Microfluidics Mixer," Review of Scientific Instruments, 80(7), pp. 075102-075102-8.
[24] Steigert, J., Grumann, M., Brenner, T., Mittenbühler, K., Nann, T., Rühe, J., Moser, I., Haeberle, S., Riegger, L., and Riegler, J., 2005, "Integrated Sample Preparation, Reaction, and Detection on a High-Frequency Centrifugal Microfluidic Platform," Journal of the Association for Laboratory Automation, 10(5), pp. 331-341.
[25] Kido, H., Micic, M., Smith, D., Zoval, J., Norton, J., and Madou, M., 2007, "A Novel, Compact Disk-Like Centrifugal Microfluidics System for Cell Lysis and Sample Homogenization," Colloids and Surfaces B: Biointerfaces, 58(1), pp. 44-51.
[26] Chakraborty, D., Madou, M., and Chakraborty, S., 2011, "Anomalous Mixing Behaviour in Rotationally Actuated Microfluidic Devices," Lab Chip, 11(17), pp. 2823-2826.
[27] Kong, M. C. R., and Salin, E. D., 2012, "Micromixing by Pneumatic Agitation on Continually Rotating Centrifugal Microfluidic Platforms," Microfluidics and Nanofluidics, pp. 1-7.
[28] Cho, H., Kim, H. Y., Kang, J. Y., and Kim, T. S., 2007, "How the Capillary Burst Microvalve Works," Journal of Colloid and Interface science, 306(2), pp. 379-385.
[29] Badr, I. H. A., Johnson, R. D., Madou, M. J., and Bachas, L. G., 2002, "Fluorescent Ion-Selective Optode Membranes Incorporated onto a Centrifugal Microfluidics Platform," Analytical Chemistry, 74(21), pp. 5569-5575.
[30] Chen, J. M., Huang, P. C., and Lin, M. G., 2008, "Analysis and Experiment of Capillary Valves for Microfluidics on a Rotating Disk," Microfluidics and Nanofluidics, 4(5), pp. 427-437.
[31] Brenner, T., Glatzel, T., Zengerle, R., and Ducree, J., 2003, "A Flow-Switch Based on Coriolis Force," Proceedings of the 7th international conference on micro total analysis systems (μTAS 2003), 2003, pp. 5-9.
[32] Kim, J., Kido, H., Rangel, R. H., and Madou, M. J., 2008, "Passive Flow Switching Valves on a Centrifugal Microfluidic Platform," Sensors and Actuators B: Chemical, 128(2), pp. 613-621.
[33] Brenner, T., Glatzel, T., Zengerle, R., and Ducrée, J., 2004, "Frequency-Dependent Transversal Flow Control in Centrifugal Microfluidics," Lab Chip, 5(2), pp. 146-150.
[34] Kong, M. C. R., and Salin, E. D., 2011, "Pneumatic Flow Switching on Centrifugal Microfluidic Platforms in Motion," Analytical Chemistry, 83(3), pp. 1148-1151.
[35] Amasia, M., Cozzens, M., and Madou, M. J., 2011, "Centrifugal Microfluidic Platform for Rapid Pcr Amplification Using Integrated Thermoelectric Heating and Ice-Valving," Sensors and Actuators B: Chemical, pp.
[36] Ukita, Y., Kondo, S., Azeta, T., Ishizawa, M., Kataoka, C., Takeo, M., and Utsumi, Y., 2012, "Stacked Centrifugal Microfluidic Device with Three-Dimensional Microchannel Networks and Multifunctional Capillary Bundle Structures for Immunoassay," Sensors and Actuators B: Chemical, pp.
[37] Gorkin, R., Soroori, S., Southard, W., Clime, L., Veres, T., Kido, H., Kulinsky, L., and Madou, M., 2012, "Suction-Enhanced Siphon Valves for Centrifugal Microfluidic Platforms," Microfluidics and Nanofluidics, pp. 1-10.
[38] Burger, R., Kirby, D., Glynn, M., Nwankire, C., O'sullivan, M., Siegrist, J., Kinahan, D., Aguirre, G., Kijanka, G., and Gorkin, R. A., 2012, "Centrifugal Microfluidics for Cell Analysis," Current Opinion in Chemical Biology, pp.
[39] Burger, J., Gross, A., Mark, D., Von Stetten, F., Zengerle, R., and Roth, G., 2011, "IR Thermocycler for Centrifugal Microfluidic Platform with Direct on-Disk Wireless Temperature Measurement System," *16th International Conf. on Solid-State Sensors, Actuators and Microsystems Conference (TRANSDUCERS), 2011*, vol., no., pp.2867-2870, 5-9 June 2011.
[40] Moore, J. L., Mccuiston, A., Mittendorf, I., Ottway, R., and Johnson, R. D., 2011, "Behavior of Capillary Valves in Centrifugal Microfluidic Devices Prepared by Three-Dimensional Printing," Microfluidics and Nanofluidics, 10(4), pp. 877-888.
[41] Kong, M. C. R., and Salin, E. D., 2011, "A Valveless Pneumatic Fluid Transfer Technique Applied to Standard Additions on a Centrifugal Microfluidic Platform," Analytical Chemistry, 83(23), pp. 9186-9190.
[42] Abi-Samra, K., Clime, L., Kong, L., Gorkin, R., Kim, T. H., Cho, Y. K., and Madou, M., 2011, "Thermo-Pneumatic Pumping in Centrifugal Microfluidic Platforms," Microfluidics and Nanofluidics, 11(5), pp. 643-652.
[43] Mark, D., Weber, P., Lutz, S., Focke, M., Zengerle, R., and Von Stetten, F., 2011, "Aliquoting on the Centrifugal Microfluidic Platform Based on Centrifugo-Pneumatic Valves," Microfluidics and Nanofluidics, 10(6), pp. 1279-1288.
[44] Wang, L., Kropinski, M. C., and Li, P. C. H., 2011, "Analysis and Modeling of Flow in Rotating Spiral Microchannels:

Towards Math-Aided Design of Microfluidic Systems Using Centrifugal Pumping," Lab on a Chip, 11(12), pp. 2097-2108.
[45] Chang, H. C., Tsou, C., Lai, C. C., and Wun, G. H., 2008, "A Real-Time Dynamic Imaging System for Centrifugal Microflow Platforms," Measurement Science and Technology, 19(7), pp. 075501.
[46] Kim, N., Dempsey, C. M., Zoval, J. V., Sze, J. Y., and Madou, M. J., 2007, "Automated Microfluidic Compact Disc (Cd) Cultivation System of *Caenorhabditis Elegans*," Sensors and Actuators B: Chemical, 122(2), pp. 511-518.
[47] Watts, A. S., Urbas, A. A., Moschou, E., Gavalas, V. G., Zoval, J. V., Madou, M., and Bachas, L. G., 2007, "Centrifugal Microfluidics with Integrated Sensing Microdome Optodes for Multiion Detection," Analytical Chemistry, 79(21), pp. 8046-8054.
[48] Puckett, L. G., Dikici, E., Lai, S., Madou, M., Bachas, L. G., and Daunert, S., 2004, "Investigation into the Applicability of the Centrifugal Microfluidics Platform for the Development of Protein-Ligand Binding Assays Incorporating Enhanced Green Fluorescent Protein as a Fluorescent Reporter," Analytical Chemistry, 76(24), pp. 7263-7268.
[49] Lai, S., Wang, S., Luo, J., Lee, L. J., Yang, S. T., and Madou, M. J., 2004, "Design of a Compact Disk-Like Microfluidic Platform for Enzyme-Linked Immunosorbent Assay," Analytical Chemistry, 76(7), pp. 1832-1837.

Appendix A

Table 1. Selected literature for application of centrifugal microfluidics

Reference	Geometry	Range of rotational speed	Area of investigation	Nature of work
Ukita et al. [36]	Detection reservoir volume = 2.8 μl, depth = 700 μm	0-2000 RPM	Multifunctional capillary bundle structures for immunoassay	Experimental
Kong et al.[27]	Chamber radius = 4 mm Chamber depth = 1.4 mm	450-1580 RPM	Pneumatic agitation on continually rotating microfluidic platform	Experimental
Kong et al. [34]	Chamber diameter = 6.35 mm Chamber depth = 1.4 mm Liquid volume = 68 μL	400-1200 RPM	Pneumatic flow switching on centrifugal microfluidic platform	Experimental
Gorkin et al. [37]	d_r = 2. 3-12.55 mm	0-6000 RPM	Suction enhanced siphon valves	Experimental and analytical
Burger et al. [38]	a = 100 μm, b = 25 μm	250-3000 RPM	Cell handling : separation and capturing/counting	Experimental
Chakraborty et al. [26]	T-microchannel a = 1 mm, b = 100 μm, L = 3.6 cm, d_r = 2.2 cm	~100-4500 RPM	Investigation of anomalous mixing behavior in rotating microchannels	Analytical and experimental
Burger et al. [39]	-	3 – 30 Hz	Infrared thermo-cycler with direct on disk wireless temperature measurement system	Experimental
Moore et al. [40]	Reservoir depth = 1 mm Valve channel dimensions a = 127, 254, 508 μm b = 254, 508, 762, 1016 μm	160-560 RPM	Behavior of capillary valves prepared by three-dimensional (solid-object) printing	Experimental
Kong et al. [41]	Capillary diameter = 75 μm	0-2600 RPM	A valveless pneumatic fluid transfer technique	Experimental
Abi-Samra et al. [42]	a = 1 mm, b = 100 μm	300-1200 RPM	Thermo-pneumatic pumping	Analytical and experimental
Mark et al. [43]	a = 400 μm, b = 200 μm	10-28 Hz Rate: 1.7 Hz/s	Aliquoting based on centrifuge-pneumatic valve	Experimental and numerical
Amasia et al. [35]	-	0-2000 RPM	PCR amplification using integrated thermo-electric heating and ice-valving	Experimental
Wang et al. [44]	d_r = 1. 9 cm (i) a = 90 μm, b = 33 μm (ii) a = 50 μm, b = 25 μm	1400-2400 RPM	Analysis and modeling of flow in rotating spiral microchannels	Analytical, numerical and experimental
Siegrist et al. [7]	Microchamber area = 75-250 mm^2 b = 200 μm	0-2000 RPM	Uniform microchamber filling behavior	Numerical and experimental
Noroozi et al. [23]	Three 240 μm-deep reservoirs, one 60 μm-deep mixing chamber, a = 60 μm, b = 240 μm	Rotating frequency = 0-24 Hz	Reciprocating flow based centrifugal microfluidics mixer	Experimental
Chakraborty et al.[19]	d_r = 2.197 cm a = 100 μm, b = 1 mm	200-700 RPM	Capillary filling with dynamically evolving contact line motion	Analytical, numerical and experi mental

Chang et al. [45]	a = 300 μm, b = 200 μm microvalve dimensions: D_h = 5 mm, b = 400 μm	0-4500 RPM	Real-time dynamic imaging system	Experimental
Liu et al. [21]	d_r = 2. 6 cm, L = 1.0cm	140-170 rad/s	Modeling of flow field, flow burst and flow timing	Analytical
Chen et al. [30]	d_r (reservoir)=2.70 cm d_r (valve)= 3.15 cm a = 300 and 400 μm b = 8-600 μm Valve expansion angle = 30°-100°	100-1000 RPM	Analysis and experiment of capillary burst valves on a rotating disk	Analytical and experimental
Kim et al. [46]	Components: a nutrient reservoir, a cultivation chamber and a waste reservoir. a = 50 μm, b = 40 μm	~227-1726 RPM Acceleration = ~17-980 m/s^2	Cultivation of *Caenorhabditis elegans* in microfluidic compact disk system	Experimental
Cho et al. [28]	d_r = 2.75 cm, a = 15-150 μm, b = 150 μm Valve expansion angle = 60°, 90°, 120°	~0-3000 RPM	Working principle of capillary burst valve	Analytical and experimental
Watts et al. [47]	a = 250-500 μm b = 200 μm	Burst frequency ~ 500-960 RPM	Multi-ion detection (Na, K, Ca, Cl) using integrated sensing microdome optodes	Experimental
Kim et al. [32]	D_h = 80 μm, a = 215 μm Δr = 1.35 cm	40-120 rad/s	Passive flow switching valves	Analytical and Experimental
Kido et al. [25]	Microchamber volume = 70 μL	50-7000 RPM	Cell lysis and sample homogenization	Experimental
Ducree et al. [16]	(i)a=100 μm, b=100 μm (ii) a=1265 μm, b=60 μm L = 2.1 cm	50-300 rad/s	Multilamination of flows in planar networks	Numerical and experimental
Ducree et al. [6]	d_r = 2.0-3.0 cm L = 2.0-2.1 cm a = 100-500 μm, b = 65-100 μm	0-150 Hz	Patterning and mixing in rotating radial microchannel	Analytical, numerical and experimental
Grumann et al. [22]	d_r = 3.9 cm mixing chamber diameter = 6 mm	~5-8 Hz	Batch-mode mixing on centrifugal microfluidic platform	Experimental
Puckett et al. [48]	Three burst valves used (i) a=635 μm , b=635 μm (ii) & (iii) a = 127 μm, b = 63.5 μm	0-1050 RPM Ramping speed = 30 RPM/s	Development of protein-ligand binding assays	Experimental
Brenner et al. [33]	a = 360 μm, b = 125 μm L = 10.1 mm	75-350 rad/s	Frequency dependent transversal flow control	Analytical and Experimental
Lai et al. [49]	a = 127-762 μm, b = 60-800 μm	360-1280 RPM	Enzyme-linked immunosorbent assay	Experimental
Madou et al. [18]	(i) a=127 μm, b=63.5 μm (ii) a=254 μm, b=127 μm (iii) a=508 μm, b=254 μm	Burst frequency ~ 524-1126 RPM	Design of a polymer based microfluidic compact disk platform	Experimental
Zeng et al. [5]	D_h = 36-250 μm	Critical burst condition, $\rho\omega^2 r\Delta r$ = 0-5000 Pa	Design analyses of capillary burst valves	Numerical and experimental
Duffy et al. [17]	D_h = 5 μm–0.5 mm b = 16 μm–3 mm	60-3000 RPM	Characterization and multiple enzymatic assays	Experimental